Electronic Supplementary Material (ESI) for Journal of Materials Chemistry A.
This journal is © The Royal Society of Chemistry 2021

Supporting Information

Significantly Enhancing Dielectric Constant and Breakdown Strength of Linear Dielectric Polymer by Ultilizing Ultralow Loadings of Nanofillers

Li Li,[ab] Jingsai Cheng,[c] Yunyun Cheng,[a] Ting Han,[a] Yang Liu,[b] Yao Zhou,[b] Zhubing Han,[b] Guanghui Zhao,[c] Yan Zhao,[c] Chuanxi Xiong,[a] Lijie Dong[a] and Qing Wang*[b]*

[a]Center for Smart Materials and Devices, State Key Laboratory of Advanced Technology for Materials Synthesis and Processing, Wuhan University of Technology, Wuhan, Hubei, 430070, P. R. China. Email: dong@whut.edu.cn

[b]Department of Materials Science and Engineering, The Pennsylvania State University, University Park, Pennsylvania 16802, USA. E-mail: wang@matse.psu.edu

[c]Research Center for Materials Genome Engineering, International Materials Science and Engineering, Wuhan University of Technology, Wuhan, Hubei, 430070, P. R. China

The classic two-component mathematical models used in this work to calculate the dielectric constant of the nanocomposites are listed as follows:

Wiener bounds model:[1]

$$\varepsilon_{\mathrm{eff}} = \varphi_{\mathrm{f}}\varepsilon_{\mathrm{f}} + \varphi_{\mathrm{m}}\varepsilon_{\mathrm{m}} \tag{1}$$

Modified Rother–Lichtenecker model:[2–4]

$$\ln \varepsilon_{\mathrm{eff}} = \ln \varepsilon_{\mathrm{m}} + \varphi_{\mathrm{f}}(1-\eta) \ln\left(\frac{\varepsilon_{\mathrm{f}}}{\varepsilon_{\mathrm{m}}}\right) \tag{2}$$

Sillars model:[5]

$$\varepsilon_{\mathrm{eff}} = \varepsilon_{\mathrm{m}}\left[1 + \frac{3\varphi_{\mathrm{f}}(\varepsilon_{\mathrm{f}}-\varepsilon_{\mathrm{m}})}{2\varepsilon_{\mathrm{m}}+\varepsilon_{\mathrm{f}}}\right] \tag{3}$$

Maxwell-Garnett model:[6–8]

$$\varepsilon_{\mathrm{eff}} = \varepsilon_{\mathrm{m}}\left[1 + \frac{3\varphi_{\mathrm{f}}(\varepsilon_{\mathrm{f}}-\varepsilon_{\mathrm{m}})}{\varphi_{\mathrm{m}}(\varepsilon_{\mathrm{f}}-\varepsilon_{\mathrm{m}})+3\varepsilon_{\mathrm{m}}}\right] \tag{4}$$

Yamada model:[9,10]

$$\varepsilon_{\mathrm{eff}} = \varepsilon_{\mathrm{m}}\left[1 + \frac{\eta\varphi_{\mathrm{f}}(\varepsilon_{\mathrm{f}}-\varepsilon_{\mathrm{m}})}{\eta\varepsilon_{\mathrm{m}}+(1-\varphi_{\mathrm{f}})(\varepsilon_{\mathrm{f}}-\varepsilon_{\mathrm{m}})}\right] \tag{5}$$

Bruggeman self-consistent effective medium approximation model:[11,12]

$$\frac{\varepsilon_{\mathrm{f}}-\varepsilon_{\mathrm{eff}}}{\varepsilon_{\mathrm{eff}}^{1/3}} = \frac{(1-\varphi_{\mathrm{f}})(\varepsilon_{\mathrm{f}}-\varepsilon_{\mathrm{m}})}{\varepsilon_{\mathrm{m}}^{1/3}} \tag{6}$$

Jaysundere-Smith model:[13]

$$\varepsilon_{\mathrm{eff}} = \frac{\varepsilon_{\mathrm{m}}\varphi_{\mathrm{m}}+\varepsilon_{\mathrm{f}}\varphi_{\mathrm{f}}\frac{3\varepsilon_{\mathrm{m}}}{2\varepsilon_{\mathrm{m}}+\varepsilon_{\mathrm{f}}}\left[1+3\varphi_{\mathrm{f}}\frac{\varepsilon_{\mathrm{f}}-\varepsilon_{\mathrm{m}}}{2\varepsilon_{\mathrm{m}}+\varepsilon_{\mathrm{f}}}\right]}{\varphi_{\mathrm{m}}+\varphi_{\mathrm{f}}\frac{3\varepsilon_{\mathrm{m}}}{2\varepsilon_{\mathrm{m}}+\varepsilon_{\mathrm{f}}}\left[1+3\varphi_{\mathrm{f}}\frac{\varepsilon_{\mathrm{f}}-\varepsilon_{\mathrm{m}}}{2\varepsilon_{\mathrm{m}}+\varepsilon_{\mathrm{f}}}\right]} \tag{7}$$

where $\varepsilon_{\mathrm{eff}}$, ε_{f} and ε_{m} are effective dielectric constant of nanocomposites, filler and polymer matrix, respectively; φ_{m} and φ_{f} are volume fractions of polymer matrix and fillers, η is a shaper factor.

The recently developed three-component interphase dielectric model used in this work to calculate the dieelctric constant of the nanocomposites is briefly descibed below:

$$K_c^{\beta} = \varphi_m K_m^{\beta} + \varphi_f K_f^{\beta} + \varphi_i K_i^{\beta} \quad (8)$$

where K_c, K_m, K_f and K_i are the K values of composite, polymer matrix, filler and interface, respectively; φ_m, φ_f and φ_i are volume fractions of polymer matrix, filler and interface, respectively; β is a filler dimension factor, for spherical fillers, β=1/3.

φ_i can be determined from the multi-core model and written as:

$$\varphi_i = \varphi_f \left[\left(1 + \frac{2t}{d}\right)^3 - 1 \right] (1 - f), f = \left(\frac{6\varphi_f}{\pi}\right)^3 \quad (9)$$

where d is the diameter of filler and t is the thickness of interface, f is a general interphase overlap probability function to evaluate the degrees of interface overlapping.

K_i can be written as:

$$K_i^{\beta} = K_m^{\beta} + \varphi_f \left(K_f^{\beta} - K_m^{\beta} \right) + \phi(\varphi_f) K_m^{\beta} \quad (10)$$

where $\phi(\varphi_f)$ represents the degree of extra enhancement of K in interface, and can be written as:

$$\phi(\varphi_f) = 1 + \frac{A}{p + (\varphi_f/\varphi_0)^q} \quad (11)$$

where $A=(K_f+qK_m)K_m^{1/2}$, φ_0 is the filling ratio where maximum K_c is achieved, p and q are matrix-determined system factors (for dipolar linear polymer, p=1, q=3).

Table S1. Summary of several dielectric parameters and predicted dielectric constants of PMMA-based nanocomposites with QDs nanofillers.

Polymer	Filler	d (nm)	K_m	K_f	φ_f	K_c (measured)	K_c (predicted)	Deviation
PMMA	QDs	7.6	3.5	10	0	3.5	3.5	0%
					0.002	4	4.4	10.0%
					0.004	4.6	5.1	10.8%
					0.006	5.3	5.6	5.6%
					0.008	5.9	5.8	−1.7%
					0.010	5.4	5.5	1.85%
					0.012	5	5	0%

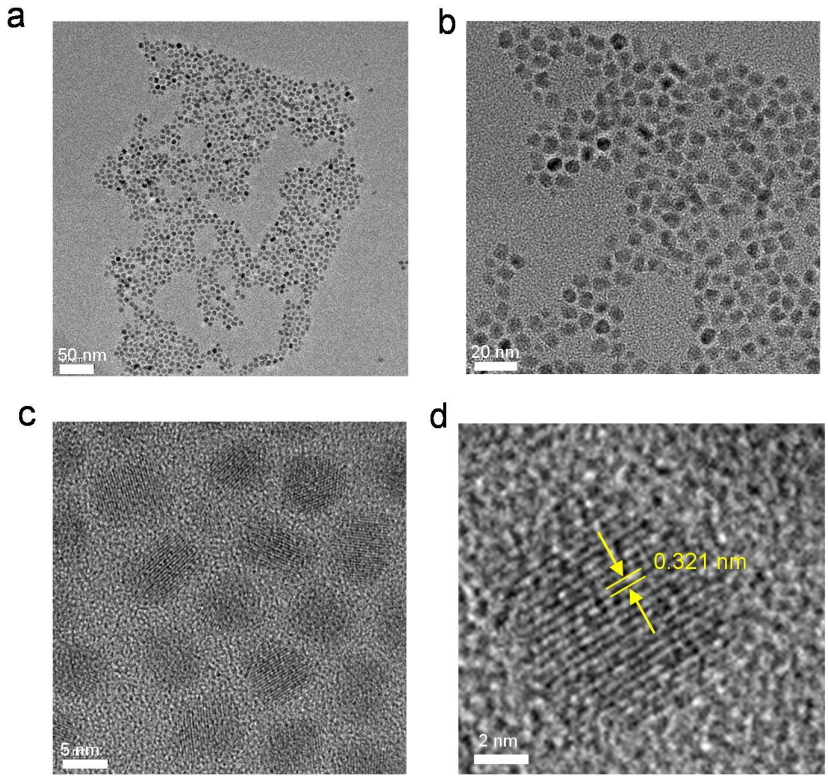

Fig. S1. TEM images of QDs. Sacle bars: a) 50 nm, b) 20 nm, c) 5 nm and d) 2 nm.

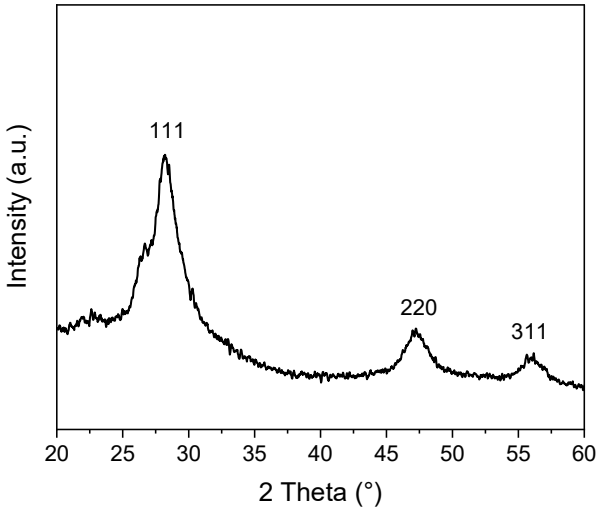

Fig. S2. XRD pattern of QDs. According to Bragg equation:

$$\lambda=2d\sin\theta \tag{12}$$

where λ is the wavelength of X-ray (Cu Kα), 0.154056 nm, d is the interplanar spacing and θ is the diffraction angel. For the (111) plane, d = 0.321 nm, which is in good agreement of HRTEM result.

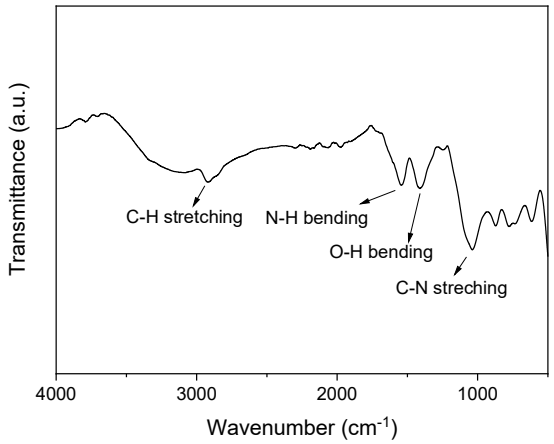

Fig. S3. FT-IR spectum of APP-functioned QDs. The peaks at 2950~2800 cm^{-1}, 1550 cm^{-1}, 1400 cm^{-1}, and 1030 cm^{-1} are corresponding to C-H stretching, N-H bending, O-H bending and C-N stretching of APP, respectively, proving that the surface structure of QDs has been modified with APP ligands.

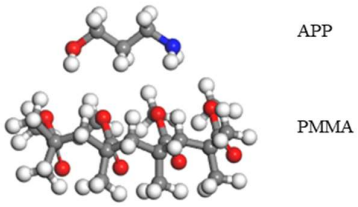

Fig. S4. DFT calculations of interaction energy, $E_{(int)}$, between PMMA and APP. Spheres colored by grey, white, cyan, red and blue represent carbon, hydrogen, fluoride, oxygen and sulfur atoms, respectively. $E_{(int)}$ is obtained as the difference between the energy of relaxed PMMA/APP complex and the original PMMA and APP, given as: $E_{(int)}=E_{(PMMA/APP)}-E_{(PMMA)}-E_{(APP)}$.

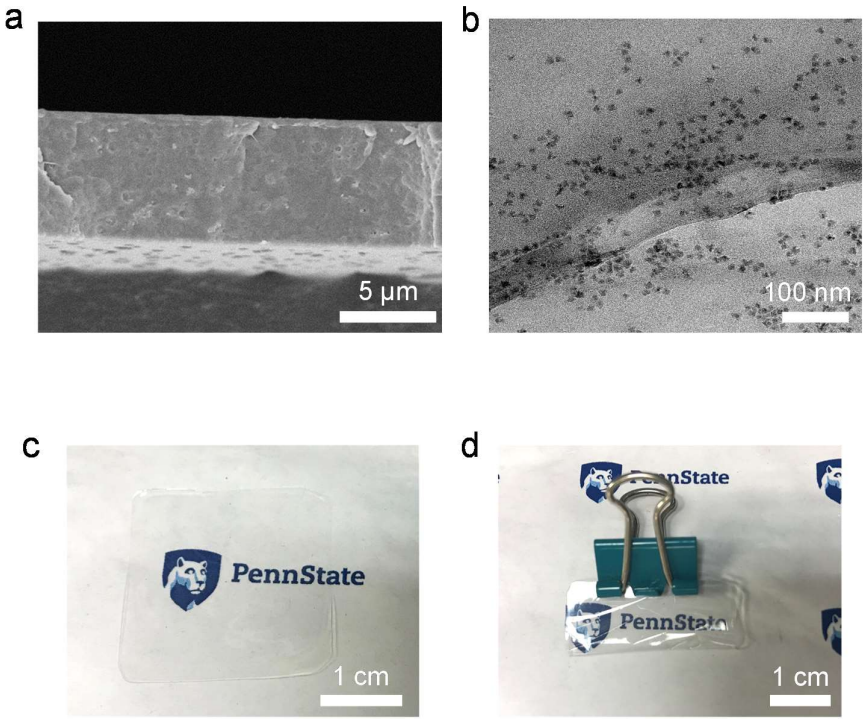

Fig. S5. a) Cross-section SEM image, b) TEM image and c, d) optical images of PMMA/QD nanocomposite films.

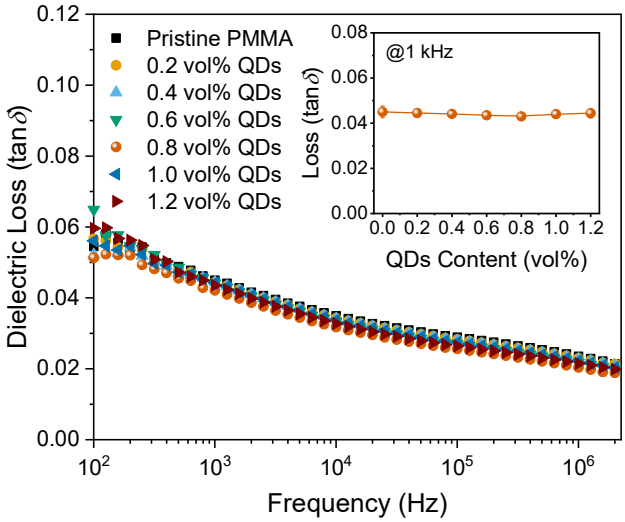

Fig. S6. Dielectric loss spectra of PMMA and PMMA/QD nanocomposites with frequency ranging from 100 Hz to 2 MHz at room temperature.

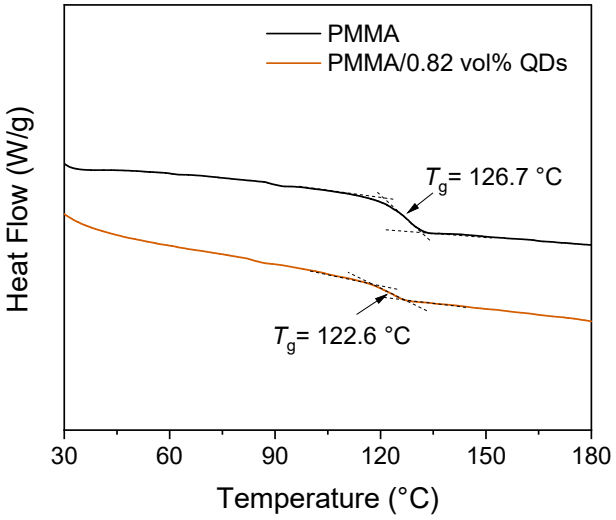

Fig. S7. DSC curves of pure PMMA and PMMA nanocomposite with 0.82 vol% QDs.

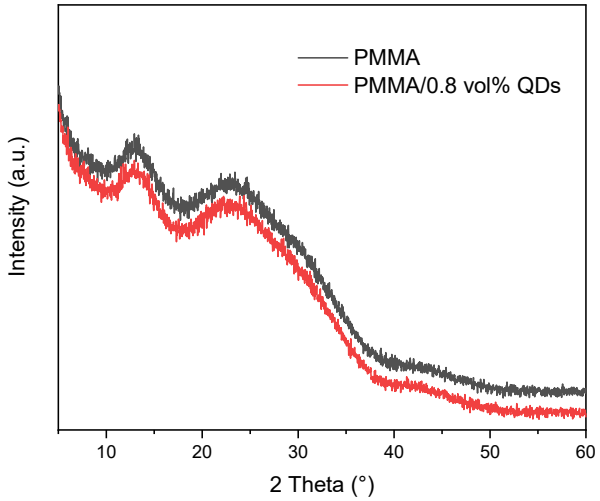

Fig. S8. XRD pateterns of pure PMMA and PMMA nanocomposite with 0.82 vol% QDs.

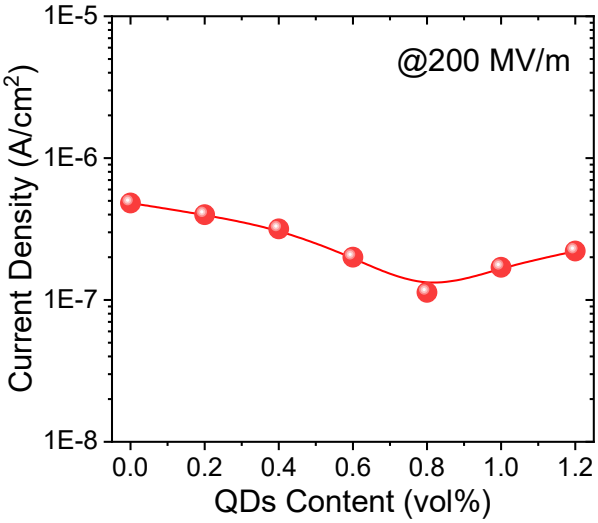

Fig. S9. Leakage current densities of PMMA and nanocomposites at 200 MV m^{-1} as a function QDs contents. The conduction loss in the nanocomposites is much suppressed than that in pure PMMA due to the numerous deep traps formed at the surface of QDs nanofillers (or the polymer-filler interfaces), which together with the enhanced mechanical strength, contributes to the largely improved E_b.[14]

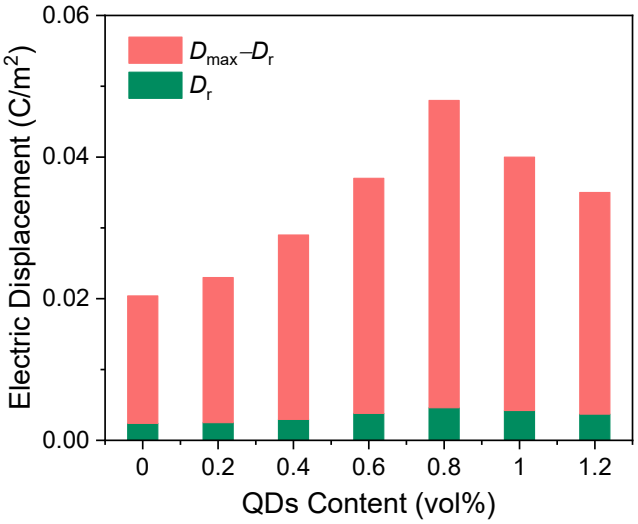

Fig. S10. Maximum and remnant electric displacement ((D_{max} and D_r) of PMMA and PMMA/QD nanocomposites with various QDs contents.

References

1 Z.-M. Dang, J.-K. Yuan, J.-W. Zha, T. Zhou, S.-T. Li and G.-H. Hu, *Prog. Mater. Sci.*, 2012, **57**, 660–723.

2 E. Brookner, *Aspects of modern radar*, Artech House on Demand, 1988.

3 K. Lichtenecker, *Phys. Z*, 1926, **27**, 115.

4 Z. Ahmad, A. Prasad and K. Prasad, *Physica B Condens. Matter.*, 2009, **404**, 3637–3644.

5 R. W. Sillars, *J. Inst. Electr. Eng.*, 1937, **80**, 378–394.

6 E. Tuncer, S. M. Gubański and B. Nettelblad, *J. Appl. Phys.*, 2001, **89**, 8092–8100.

7 S. E. Skipetrov, *Phys. Rev. B*, 1999, **60**, 12705–12709.

8 J. M. Garnett, *Philosophical Transactions of the Royal Society of London. Series A, Containing Papers of a Mathematical or Physical Character*, 1904, **203**, 385–420.

9 R. E. Newnham, D. P. Skinner and L. E. Cross, *Mater. Res. Bull.*, 1978, **13**, 525–536.

10 T. Yamada, T. Ueda and T. Kitayama, *J. Appl. Phys.*, 1982, **53**, 4328–4332.

11 A. H. Shivola, *IEEE Trans. Geosci. Remote Sens.*, 1989, **27**, 403–415.

12 V. D. Bruggeman, *Annalen der physik*, 1935, **416**, 636–664.

13 N. Jayasundere and B. V. Smith, *J. Appl. Phys.*, 1993, **73**, 2462–2466.

14 Q. Zhang, X. Chen, B. Zhang, T. Zhang, W. Lu, Z. Chen, Z. Liu, S. H. Kim, B. Donovan, R. J. Warzoha, E. D. Gomez, J. Bernholc and Q. M. Zhang, *Matter*, 2021, **4**, 2448–2459.